Hydrogen bond regulated platelet micelles by crystallization-driven self-assembly and templated growth for poly(ε-caprolactone) block copolymers

Su, Yawei; Jiang, Yikun; Liu, Liping; Xie, Yujie; Chen, Shichang; Wang, Yongjun; O'Reilly, Rachel; Tong, Zaizai

DOI:
10.1021/acs.macromol.1c02402

Document Version
Peer reviewed version

Citation for published version (Harvard):
Su, Y, Jiang, Y, Liu, L, Xie, Y, Chen, S, Wang, Y, O'Reilly, R & Tong, Z 2022, 'Hydrogen bond regulated platelet micelles by crystallization-driven self-assembly and templated growth for poly(ε-caprolactone) block copolymers', *Macromolecules*, vol. 55, no. 3, pp. 1067-1076. https://doi.org/10.1021/acs.macromol.1c02402

Hydrogen Bond Regulated Platelet Micelles by Crystallization-Driven Self-Assembly and Templated Growth for Poly(ε-Caprolactone) Block Copolymer

Yawei Su,[a,b] Yikun Jiang, [a] Liping Liu,[a,b] Yujie Xie,[c] Shichang Chen,[a] Yongjun Wang,[a] Rachel K. O'Reilly, [c] Zaizai Tong [a,b*]

a College of Materials Science and Engineering, Zhejiang Sci-Tech University, Hangzhou 310018, China

b Institute of Smart Biomedical Materials, Zhejiang Sci-Tech University, Hangzhou 310018, China

c School of Chemistry, University of Birmingham, Edgbaston, Birmingham B15 2TT, United Kingdom

Corresponding author: Tel: +86 571 86843527;

E-mail address: tongzz@zstu.edu.cn (ZT);

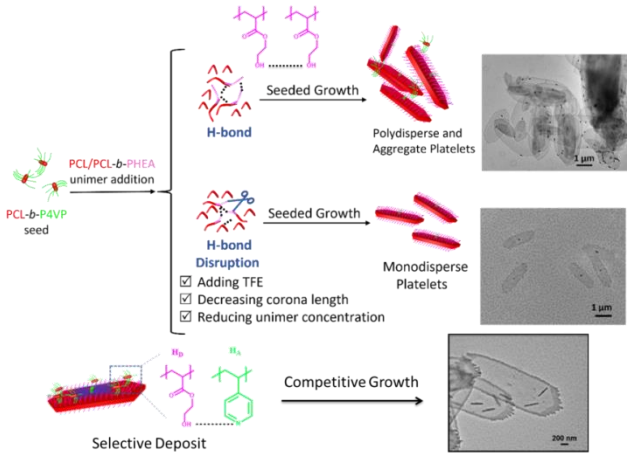

For Table of Contents use only

ABSTRACT

Living crystallization-driven self-assembly (CDSA) is a powerful approach to tailor the nanoparticles with controlled size and spatially-defined compositions from amphiphilic crystalline block copolymers (BCPs). However, a variety of external constraints usually make it difficult for the successful applications of living CDSA. Herein, such constraints arising from strong hydrogen bond (H-bond) interactions between unimers lead to the failure of living CDSA but are effectively overcome via reduction of the H-bond strength. In particular, by adding H-bond disruptor trifluoroethanol (TFE), decreasing the unimer concentration, and reducing corona segment length, the H-bond strength between unimers could be efficiently alleviated, leading to the formation of uniform two-dimensional (2D) platelets with controlled size and block co-micelles with spatially-defined corona chemistries. Moreover, by selectively anchoring 1D seeds on the surface of as-prepared 2D block co-micelles through H-bond interaction, the epitaxial growth of a crystalline BCP from immobilized 1D seeds on 2D platelets illustrates competitive growth behavior in a spatially confined environment.

INTRODUCTION

Polymer-based two-dimensional (2D) single crystals are one class of 2D nanomaterials which are usually generated from a self-nucleation methodology in a dilute solution.[1-2] However, these single crystals are generally not colloidally stable due to the low degree of functionality and absence of solvophilic groups, which further limits their potential applications.[3-5] Fortunately, recent advances in self-assembly of block copolymers (BCPs) enables access to nanostructures with different dimensions. Normally, BCPs with an amorphous core-forming block could result in spheres, worms and vesicles with core-shell structures, which are commonly predicted by packing-parameter considerations.[6] Compared to amorphous BCPs, crystalline BCPs tend to form micelles with low curvature structures in 1D or 2D through a process known as crystallization-driven self-assembly (CDSA).[7-10] Additionally, a crystalline BCP with a short corona-forming block usually forms 2D platelets, while a BCP with a significant long corona segment favors formation of 1D cylindrical micelles.[11-22] In contrast, BCPs with a biodegradable core such as poly(L-lactide) (PLLA) and poly(ε-caprolactone) (PCL) represent an opposite assembly trend, in which BCPs with long corona blocks tend to assemble into 2D platelets which is explained by "a unimer solubility approach".[23-24]

The ability to precisely control the dimensions of 2D platelets with spatially-defined chemistries is highly desirable since it can broaden the application of the 2D materials. Seeded growth, a two-step strategy separating the process of crystal nucleation and growth, provides a powerful tool to prepare monodisperse assemblies in 1D or 2D with

controlled sizes, termed as “living CDSA”. Such a strategy has been widely applied for the poly(ferrocenyldimethylsilane) (PFS) based BCPs by Manners and Winnik.[25-30] By sonicating polydisperse cylinders into short micelles as seeds, subsequent addition of dissolved BCP unimers allows epitaxial growth from the active crystalline seeds and yields monodisperse particles. For example, monodisperse 2D lenticular structures[31] or well-developed rectangular platelets[32] with spatially-defined corona chemistries can be prepared by sequentially adding symmetric PFS based BCPs, or PFS homopolymer blending with asymmetric PFS based BCPs, respectively. Up to now, the use of living CDSA strategy has been further extended to other cores, such as PCL,[33-34] PLLA,[35-37] polycarbonate,[38-39] polyethylene,[40-42] π-conjugated poly(3-thiophene),[43-44] oligo(*p*-phenylenevinylene),[45-47] and poly(cyclopentenylene vinylene).[48]

In this work, we are particularly interested in constructing 2D well-developed hierarchical complex structures of PCL core-forming BCPs using a seeded epitaxial growth process. Although the preparation of monodisperse 2D PCL platelets with controlled size has been recently reported by Stenzel’s group involving PCL homopolymer and PCL based BCP by a seeded growth process,[49] the formation of block co-micelles with spatially-defined corona chemistries and controlled dimensions has yet to be explored. Furthermore, the epitaxial crystallization of unimers from active seeds is commonly influenced by other interactions such as hydrogen bond (H-bond) and metal coordination interactions.[37, 50-51] Therefore, in this work the effect of H-bond interaction between unimers on epitaxial seeded growth was explored in detail. Generally, the presence of H-bond interaction between freshly added unimers resulted

in the formation of polydisperse platelets with extremely poor control of size. However, reducing the H-bond strength between unimers could successfully yield monodisperse 2D platelets with precise control of size. We have also successfully prepared 2D uniform block co-micelles with a segmented coronal architecture by seeded epitaxial growth after alleviating the H-bond strength. To extend to the epitaxial growth in a spatially-confined condition, the 1D seeds was selectively anchored on the surface of as-prepared 2D block co-platelets through donor-acceptor H-bond interaction. The epitaxial growth of a solely PCL based BCP from immobilized 1D seeds and as-prepared 2D platelets was finally exploited to illustrate the competitive growth of unimers in a confined environment.

RESULTS AND DISCUSSIONS

Sample Preparation and Characterizations

In the present work, three kinds of low polydispersity BCPs including PCL_{60}-*b*-$PDMA_{264}$ [PDMA = poly(*N*,*N*-dimethylacrylamide)], PCL_{60}-*b*-$P4VP_{360}$ [P4VP = poly(4-vinylpyridine)], PCL_{60}-*b*-$PHEA_{170}$ [PHEA = poly(hydroxyethyl acrylate)], were synthesized by sequential ring-opening polymerization (ROP) and reversible addition−fragmentation chain transfer (RAFT) polymerization methods (**Scheme S1**). Their chemical structures are described in **Figure 1A** and detailed molecular characterizations of all polymers are summarized in **Table S1**. The polymer characteristics were analyzed by size-exclusion chromatography (SEC) and ^{1}H NMR characterizations (**Figures S1-S6**), confirming the successful preparation of BCPs with

low dispersity. Meanwhile, the P4VP corona-forming block was chosen as H-bond acceptor, while the PHEA block served as H-bond donor and a PDMA block was used as a neutral segment (**Figure 1B**).

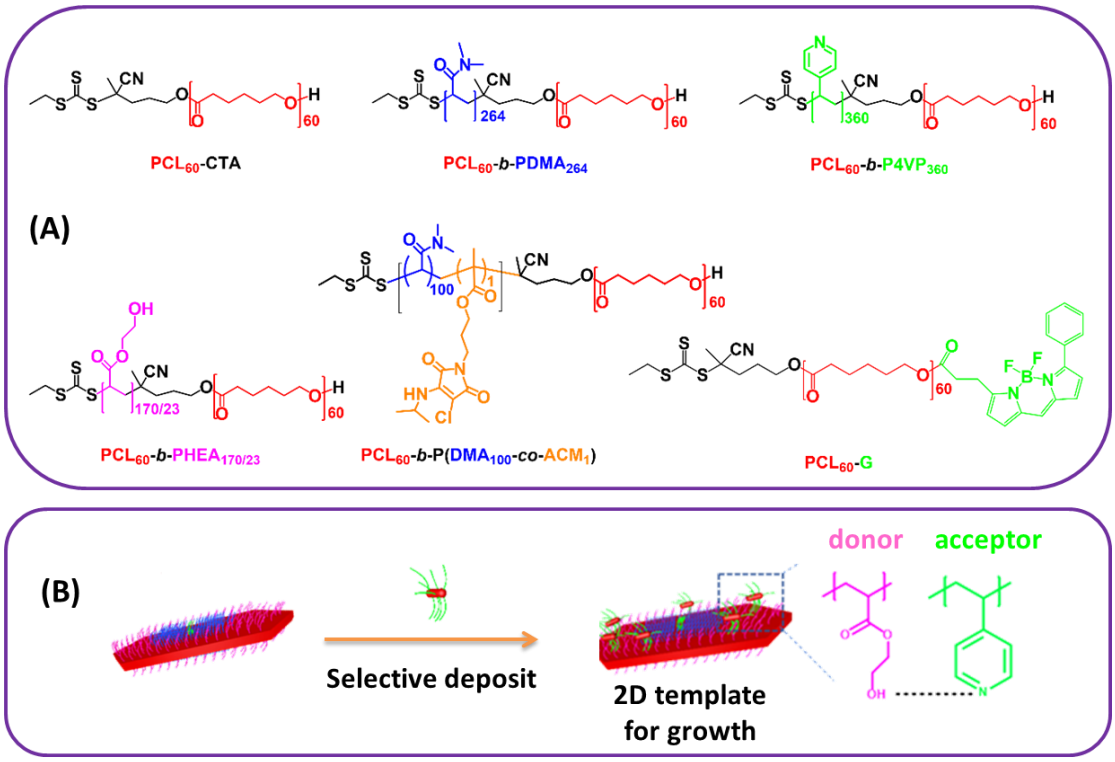

Figure 1. (A) Chemical structures of PCL homopolymers, block copolymers and dye labeled polymers used in this study and (B) construction of 2D platelets with different corona chemistries and selective deposit of 1D seeds through H-bond.

Epitaxial Growth of 2D Platelets from 1D Seeds in Ethanol

Ethanol was chosen as a selective solvent for P4VP, PDMA and PHEA corona-forming blocks, while chloroform ($CHCl_3$) was used as a good solvent for both PCL-*b*-P4VP and PCL-*b*-PDMA and dimethyl sulfoxide (DMSO) for PCL-*b*-PHEA due to high polarization of the PHEA segment. The dynamic light scattering (DLS) result showed the hydrated radius (R_h) PCL_{60}/PCL_{60}-*b*-$PDMA_{264}$ and PCL_{60}/PCL_{60}-*b*-$P4VP_{360}$ in $CHCl_3$, PCL_{60}/PCL_{60}-*b*-$PHEA_{170}$ in DMSO was about 5-10 nm (**Figure S7**),

which showed these polymer blends were fully soluble in good solvent and presented as "unimer". Polydisperse cylinders were monitored by transmission electron microscopy (TEM) from spontaneous nucleation of PCL_{60}-*b*-$P4VP_{360}$ in ethanol at a concentration of 5 mg·mL^{-1} by heating at 70 °C for 3 h and subsequently cooling to room temperature and aging for 7 days. Short cylindrical micelles with an average length of 62 nm were obtained by sonication of the polydisperse cylinders at 0 °C for 20 min, and used as seed micelles for subsequent epitaxial growth (**Figure S8**). The short 1D seed micelles of PCL_{60}-*b*-$PDMA_{264}$ were prepared by the same method and an average length of 78 nm was obtained (**Figure S9**). These seed micelles were stored at room temperature prior to epitaxial seeded growth.

To prepare uniform well-developed 2D platelets, a blend unimer of PCL homopolymer and PCL-based BCP was adopted to explore subsequent epitaxial growth in the presence of 1D PCL_{60}-*b*-$P4VP_{360}$ seed micelles. Both PCL_{60}/PCL_{60}-*b*-$P4VP_{360}$ and PCL_{60}/PCL_{60}-*b*-$PDMA_{264}$ formed well-developed platelets with controlled sizes (**Figure 2a and 2b**). It was found that blending PCL homopolymer into unimer helped to promote PCL crystallization and thus resulted in a successful seeded epitaxial growth in 2D. Such an approach has also been demonstrated in the cases of PFS based blends, indicating that incorporation of a homopolymer is a versatile method to prepare well-developed platelets with 2D structures.[32] Additionally, the surface of PCL_{60}/PCL_{60}-*b*-$PDMA_{264}$ platelets had some patterns (**Figure 2b**) while it was quite smooth for the surface of PCL_{60}/PCL_{60}-*b*-$P4VP_{360}$ platelets (**Figure 2a**). The surface patterning on platelets was attributed to coronal collapse of the relatively poorly solvated corona

segment, which was reported in detail by Manners and co-workers.[52]

However, this strategy was unsuccessful for the epitaxial seeded growth of a PCL_{60}/PCL_{60}-*b*-$PHEA_{170}$ blend unimer. Polydisperse 2D platelets with multi-layers were observed by addition of PCL_{60}/PCL_{60}-*b*-$PHEA_{170}$ blend unimer into the 1D PCL_{60}-*b*-$P4VP_{360}$ seed micelles (**Figure 2c**). In Figure 2c, a large fraction of PCL_{60}-*b*-$P4VP_{360}$ seed micelles was attached onto the surface of PCL_{60}/PCL_{60}-*b*-$PHEA_{170}$ platelets, suggesting that not all the seed micelles were serving as crystalline nuclei. Moreover, polydisperse platelets with defect-rich cores and multi-layers were also generated, which is possibly attributed to the spontaneous nucleation of PCL_{60}/PCL_{60}-*b*-$PHEA_{170}$. We preliminarily assume that such growth was caused by H-bond interaction between PCL_{60}-*b*-$P4VP_{360}$ seeds and *in-situ* formed PCL_{60}/PCL_{60}-*b*-$PHEA_{170}$ platelets, where PCL_{60}-*b*-$P4VP_{360}$ seeds served as H-bond acceptor while PCL_{60}/PCL_{60}-*b*-$PHEA_{170}$ platelets acted as H-bond donor. Therefore, we used 1D PCL_{60}-*b*-$PDMA_{264}$ seeds instead of PCL_{60}-*b*-$P4VP_{360}$ seeds to reduce the H-bond strength between 1D seed micelles and *in-situ* formed 2D platelets. However, a similar phenomenon was also monitored after addition of PCL_{60}/PCL_{60}-*b*-$PHEA_{170}$ unimer into 1D PCL_{60}-*b*-$PDMA_{264}$ seeds (**Figure S10**). A large fraction of PCL_{60}-*b*-$PDMA_{264}$ seeds was also immobilized onto the surface of platelets, which was also due to the weak H-bond interaction between PHEA and PDMA blocks. To further exclude the possibility of the effect of H-bond interaction between P4VP and PHEA blocks on subsequent epitaxial growth, PCL_{60}-*b*-$PHEA_{170}$ fragmented micelles were prepared by sonicating the polydisperse platelets as seeds. TEM observation indicated that spontaneous

nucleation strategy resulted in polydisperse platelets in 2D structures **(Figure S11)**. After sonicating the polydisperse platelets at 0 °C for 50 min, the resultant seeds preserved a fragmented platelet morphology with varying sizes and shapes (A_n=0.019 μm^2, $Đ_A$=1.26, **Figure S11c-d)**. Addition of PCL_{60}/PCL_{60}-*b*-$P4VP_{360}$ blend unimer to the PCL_{60}-*b*-$PHEA_{170}$ seed micelles allowed formation of a well-developed 2D structure with uniform size (**Figure S11e)**, indicating that the H-bond interaction between P4VP and PHEA blocks did not have a significant effect on the subsequent epitaxial growth of PCL_{60}/PCL_{60}-*b*-$P4VP_{360}$. One may doubt that these platelets were not epitaxially grown from PCL_{60}-*b*-$PHEA_{170}$ seeds since the original seed was not clearly observed in the center of platelets (**Figure S11e**), which was different from the 2D platelets observed from **Figure 2a**,**b**. This was possibly due to the phase contrast between P4VP and PHEA corona segments after stained by uranyl acetate, since the majority composition of P4VP corona was readily stained by uranyl acetate and the PHEA corona in the seeds was hard to distinguish. To further confirm the platelets were grown from the fragmented PCL_{60}-*b*-$PHEA_{170}$ seeds, control experiment was conducted. Addition of PCL_{60}/PCL_{60}-*b*-$P4VP_{360}$ blend unimer to ethanol without any seeds resulted in polydisperse platelets with multi-layers as shown **Figure S11f**.

It should be noted that a strong H-bond interaction (O-H···O, 16-21 kJ/mol) between PHEA segments also exists in ethanol. After addition of PCL_{60}/PCL_{60}-*b*-$PHEA_{170}$ blend unimer to ethanol (noting the concentration of PCL_{60}-*b*-$PHEA_{170}$ unimer is ten-fold that of seed micelles), a high concentration of PCL_{60}-*b*-$PHEA_{170}$ will exert a strong H-bond between unimers and possibly lead to unimer aggregation, which further showed

significant effect on subsequent epitaxial growth. The effect of H-bond interaction between unimers on the epitaxial growth was also observed by Manners and co-workers in the case of PLLA core based BCPs.[37] In their case, it was found that even the weak C−H···O bonds (4.2-8.4 kJ/mol) between the protons of a methyl group and the carbonyl oxygen on another polymer chain played an important role in unimer aggregation and consequential spontaneous nucleation. One should bear in mind that the H-bond strength in our case is much stronger compared to that of weak C−H···O bonds. Therefore, we try to mitigate the H-bond strength between unimers to regulate the self-assembly process.

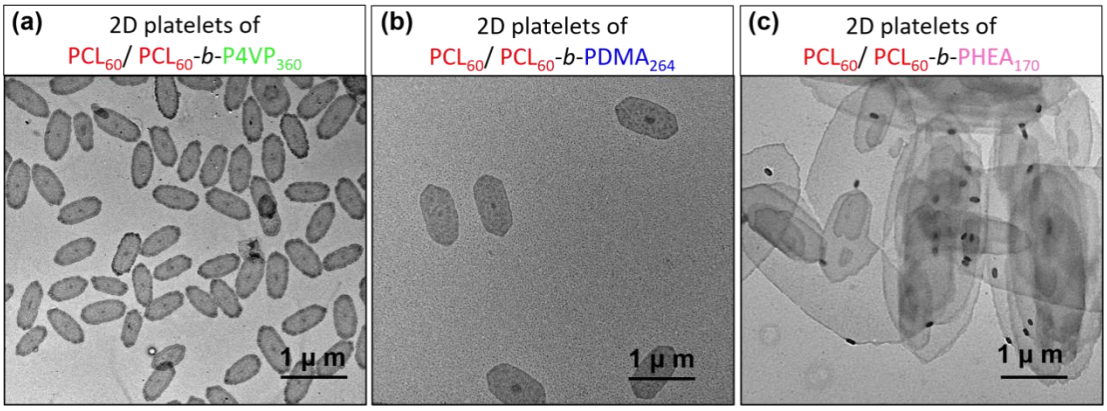

Figure 2. TEM image of 2D platelets after adding 10 μL (1:1, w/w, 10 mg·mL^{-1}) of (a) PCL_{60}/PCL_{60}-*b*-$P4VP_{360}$, (b) PCL_{60}/PCL_{60}-*b*-$PDMA_{264}$, (c) PCL_{60}/PCL_{60}-*b*-$PHEA_{170}$ blend unimer to the 1D PCL_{60}-*b*-$P4VP_{360}$ seed solution (0.01 mg·mL^{-1}, 1 mL), respectively. TEM samples were stained with a 1 wt% solution of uranyl acetate in EtOH.

Living CDSA for PCL_{60}/PCL_{60}-*b*-$PHEA_{170}$ in EtOH by Reducing H-bond Strength

To confirm the presence of strong H-bond interaction between PHEA blocks, DLS measurement was performed to illustrate the R_h change of PHEA coil by reducing the H-bond strength through adding different amount of trifluoroethanol (TFE), a hydrogen bond disruptor. To exclude the influence of PCL aggregation in ethanol, a $PHEA_{182}$

homopolymer was synthesized. As shown in **Figure S12a**, the R_h of PHEA homopolymer in ethanol decreased from 20 to 6 nm after adding more TFE. This highly suggests that the PHEA polymer chains are possibly cross-linked in ethanol due to the strong H-bond strength. However, with an increasing fraction of TFE, the R_h of PHEA homopolymer was decreased which was due to the disruption of H-bond between PHEA. Therefore, from the DLS analysis of PHEA homopolymer with the different amounts of TFE, strong H-bond interaction was indeed existed between PHEA, which had a significant effect on the subsequent seeded epitaxial growth for the PCL/PCL-*b*-PHEA. To weaken the H-bond interaction between unimers, we initially added a certain amount of TFE to the PCL_{60}-*b*-$P4VP_{360}$ seed micelle solution to explore the subsequent epitaxial growth. Blend unimer in a mass ratio of m_{unimer}/m_{seed} of 10 was added into the TFE/EtOH with volume ratios of 3/97, 5/95, 10/90, 15/85 and 20/80, respectively. After aging for 1 day, the samples were observed by TEM. As shown in **Figure S12**, the self-assembled platelets became more uniform as the TFE fraction increased, indicating that spontaneous nucleation was retarded after reducing the H-bond strength. When the volume fraction of TFE reached 20%, uniform 2D platelets with controlled size and low dispersity were formed and meanwhile the original seeds could be clearly observed in the center of platelets. Based on this factor, a living CDSA behavior of PCL_{60}/PCL_{60}-*b*-$PHEA_{170}$ in 2D was established by adding 20% volume fraction of TFE, which was confirmed by a good linear relationship between the area of the obtained platelets and m_{unimer}/m_{seed} (**Figure 3**).

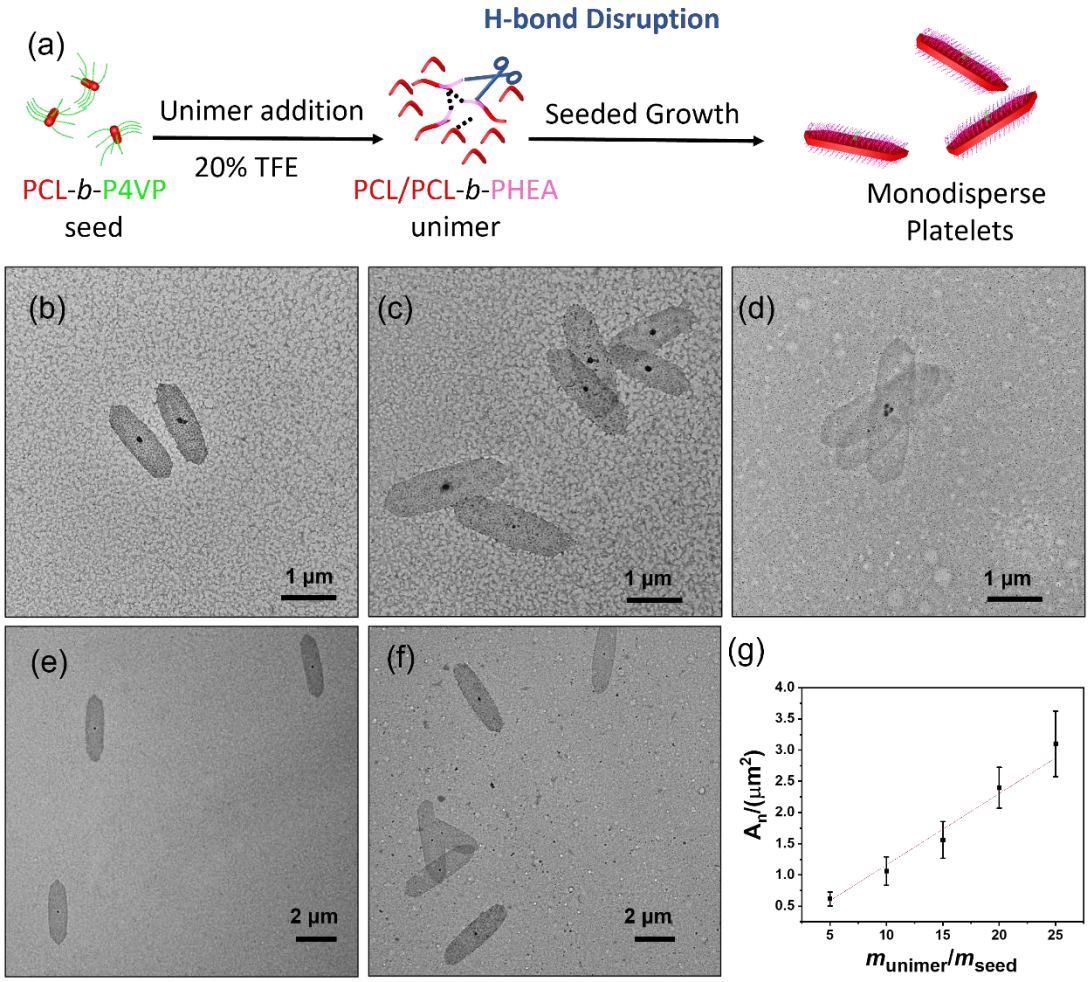

Figure 3. (a) Schematic illustration of regular platelet formation process by adding 20% volume TFE; TEM image of 2D platelets with various area obtained by adding (b) 5 μL, (c) 10 μL, (d) 15 μL, (e) 20 μL, (f) 25 μL of PCL_{60}/PCL_{60}-*b*-$PHEA_{170}$ (1:1, w/w, 10 mg·mL^{-1}) unimer solution in DMSO to the 1D PCL_{60}-*b*-$P4VP_{360}$ seed solution (0.01 mg·mL^{-1}, 1 mL) with 20% TFE; (g) plot of number-average area of 2D platelet against m_{unimer}/m_{seed} (the error bars represent the standard deviation). TEM samples were stained with a 1 wt% solution of uranyl acetate in EtOH.

It is well known that TFE is a strong organic acid, which possibly will exert a certain corrosive effect on PCL platelets since the biodegradable PCL core has a fast degradation rate in an acid environment. For this reason, the stability of as-prepared uniform platelets in TFE/EtOH was examined. As shown in **Figure S13**, the obtained uniform 2D platelets did not change significantly after 1 day but degraded to some

extent after 7 days in TFE/EtOH, suggesting that TFE accelerated the degradation rate of the PCL core. Considering this factor, we tried to remove TFE by rotary evaporating at room temperature and then adding the same volume of EtOH to re-disperse the platelets. Unfortunately, the uniform platelets were easily stacked together after removing TFE, which was due to strong H-bond interaction of the platelets between PHEA corona segments **(Figure S13c)**. This forced us to explore other self-assembly conditions to overcome this potential problem.

As mentioned above, the H-bond strength between unimers is the key factor to determine final self-assembled platelets. Reducing the H-bond strength between unimers could help to form uniform platelets such as addition of a certain amount of TFE. Based on this fact, we prepared another BCP with a short PHEA block, PCL_{60}-*b*-$PHEA_{23}$, to reduce the H-bond strength between unimers. As expected, well-developed platelets with low polydispersity in size were formed after addition of PCL_{60}/PCL_{60}-*b*-$PHEA_{23}$ blend unimer in the presence of 1D PCL_{60}-*b*-$P4VP_{360}$ seed micelles (**Figure 4a)**. On the other hand, decreasing the concentration of the PCL_{60}-*b*-$PHEA_{170}$ unimer could also reduce the H-bond strength between PCL_{60}-*b*-$PHEA_{170}$ unimer in ethanol. Therefore, we diluted the concentration of seed micelles from 0.01 to 0.001 $mg{\cdot}mL^{-1}$ and subsequently added 1 μL of PCL_{60}/PCL_{60}-*b*-$PHEA_{170}$ (1:1, w/w, 10 $mg{\cdot}mL^{-1}$) unimer solution to the diluted 1D PCL_{60}-*b*-$P4VP_{360}$ seed solution (0.001 $mg{\cdot}mL^{-1}$, 1 mL), resulting in well-developed 2D platelets with low polydispersity in size (**Figure 4b**). This method of decreasing the unimer concentration was also applied to prepare 2D diblock co-micelles. As shown in **Figure 4c**, dropping 3 μL of PCL_{60}/PCL_{60}-*b*-

$PHEA_{170}$ (1:1, w/w, 10 mg·mL^{-1}) blend unimer onto 2D platelets of PCL_{60}/PCL_{60}-*b*-PDA_{264} (0.01 mg·mL^{-1}, 1 mL) in ethanol also promoted formation of 2D block co-micelles with low polydispersity in size. Meanwhile, the two spatially-defined regions of the diblock co-micelles were clearly distinguishable by TEM analysis.

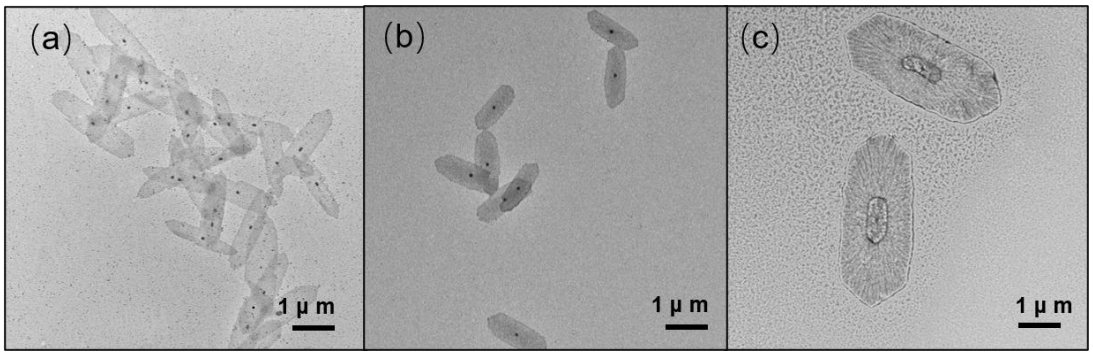

Figure 4. TEM image of 2D platelets obtained by (a) adding 10 μL of PCL_{60}/PCL_{60}-*b*-$PHEA_{23}$ (1:1, w/w, 10 mg·mL^{-1}) blend unimer solution to the 1D PCL_{60}-*b*-$P4VP_{360}$ seed solution (0.01 mg·mL^{-1}, 1 mL) without TFE and (b) adding 1 μL of PCL_{60}/PCL_{60}-*b*-$PHEA_{170}$ (1:1, w/w, 10 mg·mL^{-1}) blend unimer solution to the diluted 1D PCL_{60}-*b*-$P4VP_{360}$ seed solution (0.001 mg·mL^{-1}, 1 mL) without TFE. (c) Addition of 3 μL of PCL_{60}/PCL_{60}-*b*-$PHEA_{170}$ (1:1, w/w, 10 mg·mL^{-1}) blend unimer to 2D platelet of PCL_{60}/PCL_{60}-*b*-$PDMA_{264}$ (0.01 mg·mL^{-1}, 1 mL) in EtOH. TEM samples were stained with a 1 wt% solution of uranyl acetate in EtOH.

Construction of Block Co-Micelles

The successful access to efficient living CDSA of PCL_{60}/PCL_{60}-*b*-$PHEA_{170}$ allows us to prepare complex structures in 2D with well-defined spatial localization of different coronal chemistries, which endows the nanoparticles with more functionality. After successfully accomplishing the 2D epitaxial growth using 1D short seeds, we then targeted use of the resulting 2D platelets as seed precursors for subsequent epitaxial growth of a second platelet on the platelet edges (**Figure 5** and **Figure S14-S15**). Addition of PCL_{60}/PCL_{60}-*b*-$PDMA_{264}$ blend unimer to 2D precursors of PCL_{60}/PCL_{60}-*b*-$PHEA_{170}$ resulted in 2D diblock co-micelles containing two different regions with

inner region as PHEA corona while the outer segment as PDMA corona (**Figure 5a**). By labelling the PCL_{60} homopolymer core with BODIPY green dye (PCL_{60}-G, **Figure 1A**), living CDSA of the blend of PCL_{60}-G/PCL_{60}-*b*-$PDMA_{264}$ yielded green fluorescent concentric platelet block co-micelles (**Figure 5b**) as confirmed with confocal laser scanning microscopy (CLSM). On the other hand, we can also use 2D platelets of PCL_{60}/PCL_{60}-*b*-$PDMA_{264}$ as precursors to initiate the epitaxial growth of PCL_{60}/PCL_{60}-*b*-$PHEA_{170}$ or PCL_{60}/PCL_{60}-*b*-$PHEA_{23}$ blend unimer. Both of them formed well-developed and monodisperse diblock co-micelles in 2D (**Figure 5c,d**) under a low unimer concentration, demonstrating a powerful method that involves seeded growth of a polymer blend by reducing H-bond strength.

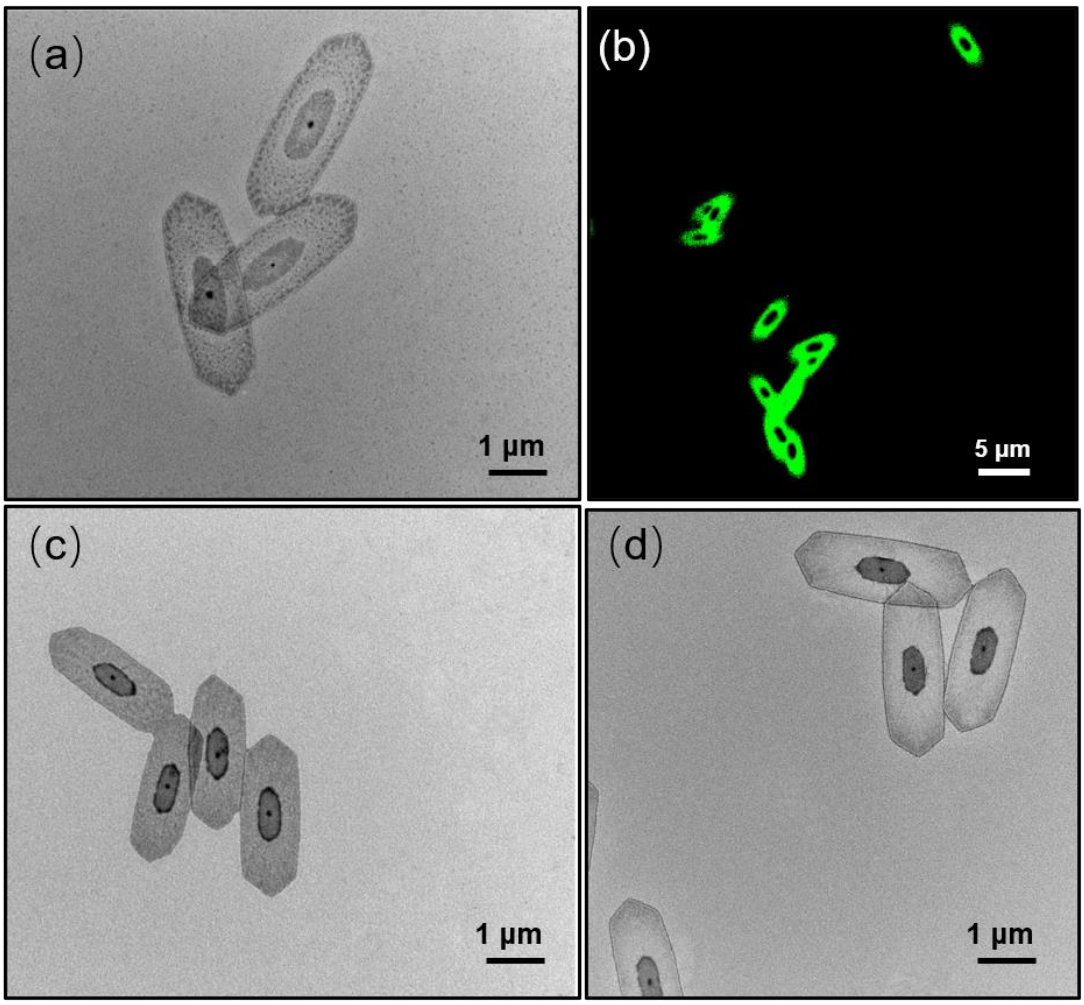

Figure 5. (a) TEM and (b) corresponding CLSM image of 2D diblock co-micelles yielded by adding 3 μL of PCL_{60}-G/PCL_{60}-*b*-$PDMA_{264}$ (1:1, w/w, 10 mg·mL^{-1}) blend unimer solution to the 2D PCL_{60}/PCL_{60}-*b*-$PHEA_{170}$ seed solution (0.01 mg·mL^{-1}, 1 mL). TEM image of 2D diblock co-micelles obtained by adding 3 μL of (c) PCL_{60}/PCL_{60}-*b*-$PHEA_{170}$ (1:1, w/w, 10 mg·mL^{-1}) blend unimer solution and (d) PCL_{60}/PCL_{60}-*b*-$PHEA_{23}$ (1:1, w/w, 10 mg·mL^{-1}) blend unimer solution to the 2D PCL_{60}/PCL_{60}-*b*-$PDMA_{264}$ seed solution (0.01 mg·mL^{-1}, 1 mL), respectively. TEM samples were stained with a 1 wt% solution of uranyl acetate in EtOH.

Furthermore, well-defined and monodisperse concentric 2D structures containing P4VP, PHEA and PDMA corona segments separated by distinct boundaries were successfully prepared by sequential addition of PCL_{60}/PCL_{60}-*b*-$P4VP_{360}$, PCL_{60}/PCL_{60}-*b*-$PHEA_{170}$ and PCL_{60}/PCL_{60}-*b*-$PDMA_{264}$ blend unimers into 1D PCL_{60}-*b*-$P4VP_{360}$ seed micelles (**Figure 6**). As a proof-of-concept, another fluorescent sample PCL_{60}-*b*-P(DMA_{100}-*co*-ACM_1) was prepared (**Figure 1A**), in which the PDMA corona segment was functionalized with aminochloromaleimide (ACM dye [53-54]) by copolymerization (**Scheme S1**). Living CDSA of fluorescent blends, i.e., PCL_{60}-G/PCL_{60}-*b*-$P4VP_{360}$ and PCL_{60}/PCL_{60}-*b*-P(DMA_{100}-*co*-ACM_1), together with the non-fluorescent PCL_{60}/PCL_{60}-*b*-$PHEA_{170}$ blends, yielded fluorescent concentric platelet block co-micelles with different fluorescence for the selected segments, as confirmed by CLSM (**Figure 6d**). Further deposition was also feasible by using the spatially-defined corona chemistries. For instance, 1D PCL_{60}-*b*-$P4VP_{360}$ seed micelles were selectively deposited onto the PHEA coronas' regions (middle region) as a result of the O-H···N bond interaction (**Figure 6e**).

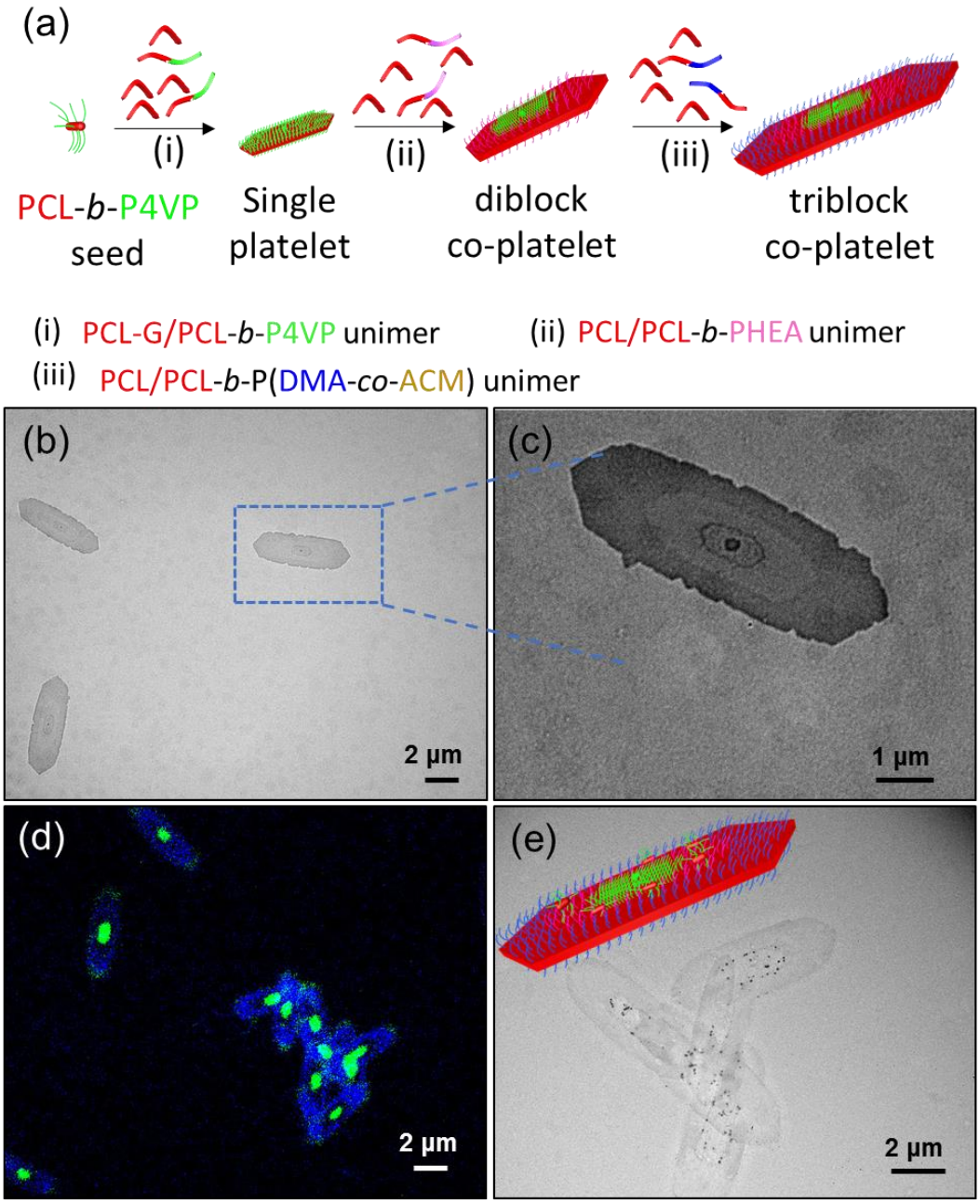

Figure 6. (a) Schematic illustration of preparation of triblock co-micelles. (b) TEM image of 2D triblock co-platelets prepared by sequential addition of PCL_{60}-G/PCL_{60}-*b*-$P4VP_{360}$, PCL_{60}/PCL_{60}-*b*-$PHEA_{170}$ and PCL_{60}/PCL_{60}-*b*-P(DMA_{100}-*co*-ACM_1) blend unimers into 1D PCL_{60}-*b*-$P4VP_{360}$ seed micelles. (c) Enlarged one platelet co-micelles with distinct platelet boundaries. (d) CLSM image of dye labeled platelet co-micelles. The inner region (P4VP region, green): PCL core was labeled with BODIPY green dye; the outer region (PDMA region, blue): the PDMA corona was labeled with ACM dye. (e) TEM images of triblock co-micelles with 1D PCL_{60}-*b*-$P4VP_{360}$ seed micelles selectively deposited on the PHEA coronas (middle region) through O-H···N bond. TEM samples were stained with a 1 wt% solution of uranyl acetate in EtOH.

Exploring the Seeded Growth of Solely PCL_{60}-*b*-$P4VP_{360}$ from a 2D Template

In this section, we planned to explore the seeded growth of PCL_{60}-*b*-$P4VP_{360}$ by anchoring 1D PCL_{60}-*b*-$P4VP_{360}$ seeds onto 2D templates containing PHEA corona through O-H···N bond interaction. For a deep understanding, we first used 2D graphene oxide (GO) nanosheets as a template to immobilize the 1D PCL_{60}-*b*-$P4VP_{360}$ seeds to explore the subsequent epitaxial growth of PCL_{60}-*b*-$P4VP_{360}$. Our attempt is to show whether the seeded growth of PCL_{60}-*b*-$P4VP_{360}$ will be restricted by both the spatial confinement exerted from GO nanosheets and H-bond interaction between GO and PCL_{60}-*b*-$P4VP_{360}$ unimer. For better comparison, the seeded growth of solely PCL_{60}-*b*-$P4VP_{360}$ unimer from 1D seeds without any template in ethanol was first examined. As shown in **Figure S16** and **Figure S17**, the morphology including the average length of PCL_{60}-*b*-$P4VP_{360}$ epitaxially grown from 1D seeds anchored on the GO surface did not change significantly compared to that without a GO template, suggesting that the presence of GO had negligible effect on the following epitaxial growth. Meanwhile, the resultant crystals grown at a high m_{unimer}/m_{seed} value (such as 15 and 20) tended to form a lenticular morphology in 2D (**Figures S16c,d** and **S17c,d**) similar to previously reported lenticular assemblies.[31, 55] On the other hand, addition of solely PCL_{60}-*b*-$P4VP_{360}$ unimer to the 2D PCL_{60}/PCL_{60}-*b*-$PDMA_{264}$ platelets in ethanol led to "platelet-fiber" structure with a high density of fibers grown from the four (110) crystalline planes of PCL platelets (**Figure S18**). A living growth of PCL_{60}-*b*-$P4VP_{360}$ unimer from 2D PCL platelets was also established as demonstrating by a linear relationship between the length of cylinders and the added unimers (**Figure S18**). High magnification TEM

images (**Figure S18g'**) showed these fibers had a uniform width and the length could reach to about 1000 nm, which was different from the morphology grown from free 1D seeds. This result strongly confirmed the essential growth of solely PCL_{60}-*b*-$P4VP_{360}$ unimer in 1D nucleated from 2D platelets, which was possibly attributed to the strong spatial confinement exerted by a high nucleation density. Similar phenomenon was also observed in our previous result by anchoring 1D seeds onto carbon nanotube at a high grafting density.[33]

Next, we aimed to explore the seeded growth of PCL_{60}-*b*-$P4VP_{360}$ by anchoring 1D PCL_{60}-*b*-$P4VP_{360}$ seed micelles on the surface of 2D block co-micelles by utilizing the O-H···N bond interaction between PHEA (H-bond donor, H_D) and P4VP (H-bond acceptor, H_A) with a fixing ratio of pyridine/hydroxyl group (0.2:1). This targeted creation of a severe confinement for epitaxial growth of PCL_{60}-*b*-$P4VP_{360}$ unimer from the immobilized seeds. After selectively depositing 1D seeds on the PHEA region of diblock co-micelles containing an inner PDMA corona and outer PHEA corona (**Figure 7a, b**), the epitaxial growth of solely PCL_{60}-*b*-$P4VP_{360}$ unimer was explored by addition of increasing amounts of PCL_{60}-*b*-$P4VP_{360}$ unimer (**Figure 7c-g**). PCL_{60}-*b*-$P4VP_{360}$ unimer was preferentially deposited onto the end of 2D platelets when only a small amount of PCL_{60}-*b*-$P4VP_{360}$ was added. This allowed formation of a "platelet-cylinder" structure with quasi-linear tassels of about 25 nm at both ends since the length of the cylinders immobilized on the platelet does not increase (60 nm compared to 62 nm of seeds). As the amount of added PCL_{60}-*b*-$P4VP_{360}$ unimer increased, both the length of tassels and cylinders anchored on the platelets increased. However, the increasing

growth rate of cylinders from 2D platelets was slower than that from immobilized 1D seeds since the growing slope was smaller than that from 1D seeds as confirmed by **Figure 7h**, possibly due to strong spatial confinement exerted by a high nucleation density from both ends of 2D platelets. Meanwhile, the formed cylinders from immobilized 1D seeds were also essentially grown into 1D structure even the length exceeded 500 nm (**Figure 7g**), demonstrating that the strong H-bond strength between PCL-*b*-P4VP unimer and PHEA corona segment of 2D platelets could affect the crystal growth behavior of PCL_{60}-*b*-$P4VP_{360}$. This change of epitaxial growth possibly results from the reducing mobility of PCL_{60}-*b*-$P4VP_{360}$ unimer exerted by H-bond when deposited on the active seeds, which is very similar to the effect of metal ion complexation between corona observed by Feng and co-workers.[50]

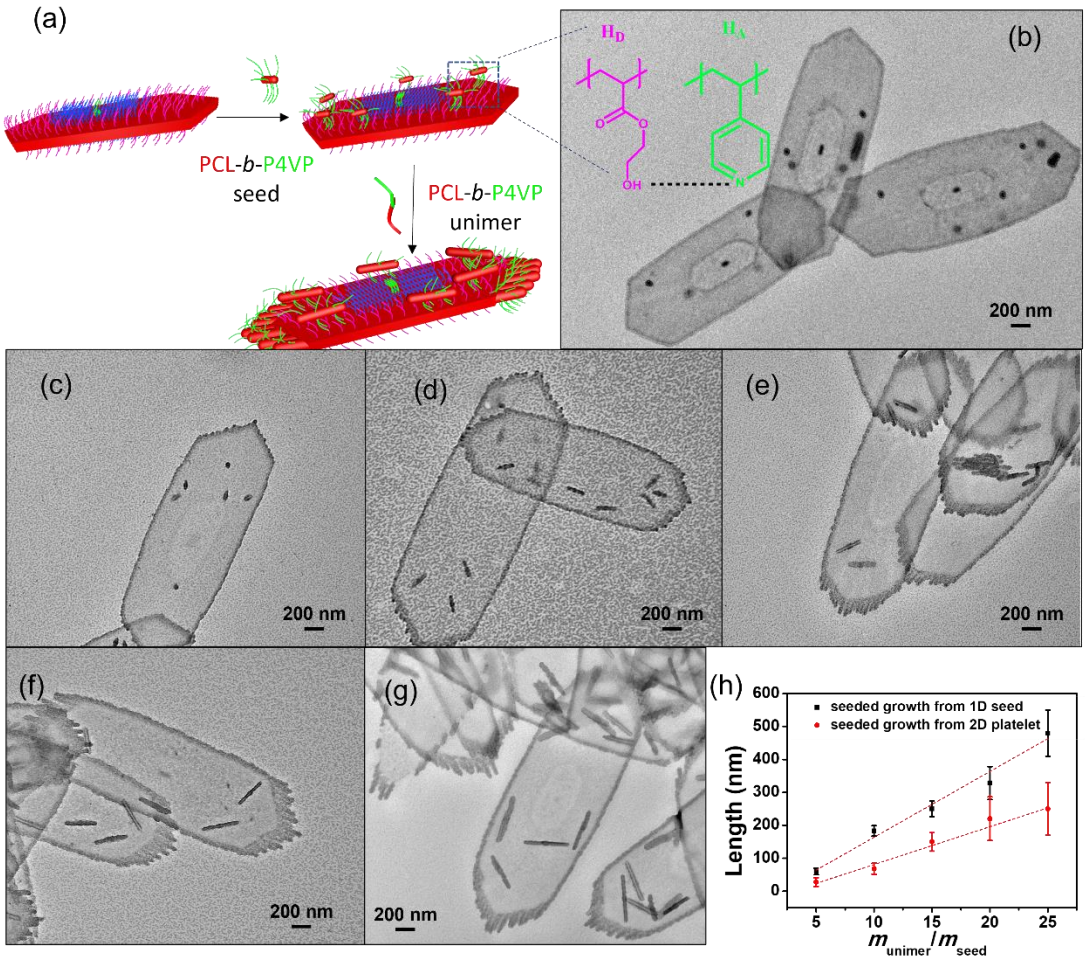

Figure 7. (a) Schematic representation of epitaxial growth of PCL_{60}-*b*-$P4VP_{360}$ from a template of 2D platelet with anchored 1D PCL_{60}-*b*-$P4VP_{360}$ seeds (inner: PDMA region, blue corona; outer: PHEA region, pink corona); (b) TEM image of selective deposition of PCL_{60}-*b*-$P4VP_{360}$ seeds on the PHEA surface prepared by sequential addition of PCL_{60}/PCL_{60}-*b*-$PDMA_{264}$ and PCL_{60}/PCL_{60}-*b*-$PHEA_{170}$ blend unimers in the presence of 1D PCL_{60}-*b*-$P4VP_{360}$ seeds. TEM images of addition of (c) 3 μL, (d) 6 μL, (e) 9 μL, (f) 12 μL, (g) 15 μL of solely PCL_{60}-*b*-$P4VP_{360}$ (10 mg·mL^{-1}) unimer solution to the above formed 2D template in (b) (mass of PCL_{60}-*b*-$P4VP_{360}$ seed is 0.006 mg); (h) Plots of number-average 1D quasi-linear cylindrical micelles length against m_{unimer}/m_{seed} from 1D seeds and 2D platelets (the error bars represent the standard deviation), respectively. TEM samples were stained by the 1 wt% solution of uranyl acetate in EtOH.

CONCLUSIONS

To summarize, an efficient living CDSA approach was established by reducing the H-bond strength between PHEA unimers. Methods including the addition of a hydrogen bond disruptor, decreasing the unimer concentration, and reducing corona segment

length were applied to mitigate H-bond strength. By utilizing these strategies, we have successfully prepared a variety of 2D platelets with controlled size and also achieved multi-block co-micelles with spatially-defined corona chemistries. Our results have demonstrated that the use of analogous approaches is potentially effective for the systems in which living CDSA behavior has been inefficient to date such as exerting strong external interaction. As part of our studies, we also revealed the restricted epitaxial growth and competitive epitaxial growth of PCL_{60}-*b*-$P4VP_{360}$. The result showed that strong confinement exerted by 2D platelets could affect the crystal growth behavior of PCL_{60}-*b*-$P4VP_{360}$ unimer probably due to the reduced mobility of PCL_{60}-*b*-$P4VP_{360}$ chain.

ASSOCIATED CONTENT

Supporting Information

The Supporting Information is available free of charge on the ACS Publications website. Additional experimental details, characterization data, results and discussion, and supporting figures (PDF).

AUTHOR INFORMATION

Acknowledgements

This work was financially supported by the National Natural Science Foundation of China (21604073, 52173047) and Shaoxing City Science and Technology Program (2020B21001).

AUTHOR INFORMATION

Corresponding Author

*E-mail: tongzz@zstu.edu.cn (ZT)

Conflict of Interest

The authors declare no conflict of interest.

REFERENCES

(1) Chiang, Y.-W.; Hu, Y.-Y.; Li, J.-N.; Huang, S.-H.; Kuo, S.-W. Trilayered Single Crystals with Epitaxial Growth in Poly(Ethylene Oxide)-*block*-Poly(ε-Caprolactone)-*block*-Poly(*L*-Lactide) Thin Films. *Macromolecules* **2015**, *48* (23), 8526-8533.

(2) Agbolaghi, S.; Abbaspoor, S.; Abbasi, F. A Comprehensive Review on Polymer Single Crystals-from Fundamental Concepts to Applications. *Prog. Polym. Sci.* **2018**, *81*, 22-79.

(3) Dong, B.; Miller, D. L.; Li, C. Y. Polymer Single Crystal as Magnetically Recoverable Support for Nanocatalysts. *J. Phys. Chem. Lett.* **2012**, *3* (10), 1346-1350.

(4) Shi, L.; Liu, M.; Liu, L.; Gao, W.; Su, M.; Ge, Y.; Zhang, H.; Dong, B. Magnetically Recyclable Polymer Single Crystal Supported Silver Nanocatalyst. *Langmuir* **2014**, *30* (44), 13456-13461.

(5) Wu, J.; Weng, L.-T.; Qin, W.; Liang, G.; Tang, B. Z. Crystallization-Induced Redox-Active Nanoribbons of Organometallic Polymers. *ACS Macro Lett.* **2015**, *4* (5), 593-597.

(6) Mai, Y.; Eisenberg, A. Self-Assembly of Block Copolymers. *Chem. Soc. Rev.* **2012**,

41 (18), 5969-5985.

(7) He, W. N.; Xu, J. T. Crystallization Assisted Self-Assembly of Semicrystalline Block Copolymers. *Prog. Polym. Sci.* **2012**, *37* (10), 1350-1400.

(8) Ganda, S.; Stenzel, M. H. Concepts, Fabrication Methods and Applications of Living Crystallization-Driven Self-Assembly of Block Copolymers. *Prog. Polym. Sci.* **2020**, *101*, 101195.

(9) MacFarlane, L.; Zhao, C.; Cai, J.; Qiu, H.; Manners, I. Emerging Applications for Living Crystallization-Driven Self-Assembly. *Chem. Sci.* **2021**, *12* (13), 4661-4682.

(10) Hils, C.; Manners, I.; Schobel, J.; Schmalz, H. Patchy Micelles with a Crystalline Core: Self-Assembly Concepts, Properties, and Applications. *Polymers* **2021**, *13* (9), 1481.

(11) Zheng, J. X.; Xiong, H.; Chen, W. Y.; Lee, K.; Van Horn, R. M.; Quirk, R. P.; Lotz, B.; Thomas, E. L.; Shi, A.-C.; Cheng, S. Z. D. Onsets of Tethered Chain Overcrowding and Highly Stretched Brush Regime via Crystalline−Amorphous Diblock Copolymers. *Macromolecules* **2006**, *39* (2), 641-650.

(12) Du, Z. X.; Xu, J. T.; Fan, Z. Q. Micellar Morphologies of Poly(ε-Caprolactone)-*b*-Poly(Ethylene Oxide) Block Copolymers in Water with a Crystalline Core. *Macromolecules* **2007**, *40* (21), 7633-7637.

(13) He, W. N.; Zhou, B.; Xu, J. T.; Du, B. Y.; Fan, Z. Q. Two Growth Modes of Semicrystalline Cylindrical Poly(ε-Caprolactone)-*b*-Poly(Ethylene Oxide) Micelles. *Macromolecules* **2012**, *45* (24), 9768-9778.

(14) Fan, B.; Wang, R. Y.; Wang, X. Y.; Xu, J. T.; Du, B. Y.; Fan, Z. Q. Crystallization-Driven Co-Assembly of Micrometric Polymer Hybrid Single Crystals and Nanometric Crystalline Micelles. *Macromolecules* **2017**, *50* (5), 2006-2015.

(15) Fan, B.; Xue, J.-Q.; Guo, X.-S.; Cao, X.-H.; Wang, R.-Y.; Xu, J.-T.; Du, B.-Y.; Fan, Z.-Q. Regulated Fragmentation of Crystalline Micelles of Block Copolymer Via Monoamine-Induced Corona Swelling. *Macromolecules* **2018**, *51* (19), 7637-7648.

(16) Wang, X.-Y.; Wang, R.-Y.; Fan, B.; Xu, J.-T.; Du, B.-Y.; Fan, Z.-Q. Specific Disassembly of Lamellar Crystalline Micelles of Block Copolymer into Cylinders. *Macromolecules* **2018**, *51* (5), 2138-2144.

(17) Wang, J.; Zhu, W.; Peng, B.; Chen, Y. A Facile Way to Prepare Crystalline Platelets of Block Copolymers by Crystallization-Driven Self-Assembly. *Polymer* **2013**, *54* (25), 6760-6767.

(18) Tong, Z.; Li, Y.; Xu, H.; Chen, H.; Yu, W.; Zhuo, W.; Zhang, R.; Jiang, G. Corona Liquid Crystalline Order Helps to Form Single Crystals When Self-Assembly Takes Place in the Crystalline/Liquid Crystalline Block Copolymers. *ACS Macro Lett.* **2016**, *5* (7), 867-872.

(19) Tong, Z.; Zhang, R.; Ma, P.; Xu, H.; Chen, H.; Li, Y.; Yu, W.; Zhuo, W.; Jiang, G. Surfactant-Mediated Crystallization-Driven Self-Assembly of Crystalline/Ionic Complexed Block Copolymers in Aqueous Solution. *Langmuir* **2017**, *33* (1), 176-183.

(20) Foster, J. C.; Varlas, S.; Couturaud, B.; Coe, Z.; O'Rei'lly, R. K. Getting into Shape: Reflections on a New Generation of Cylindrical Nanostructures' Self-Assembly

Using Polymer Building Blocks. *J. Am. Chem. Soc.* **2019**, *141* (7), 2742-2753.

(21) Song, S.; Yu, Q.; Zhou, H.; Hicks, G.; Zhu, H.; Rastogi, C. K.; Manners, I.; Winnik, M. A. Solvent Effects Leading to a Variety of Different 2D Structures in the Self-Assembly of a Crystalline-Coil Block Copolymer with an Amphiphilic Corona-Forming Block. *Chem. Sci.* **2020**, *11* (18), 4631-4643.

(22) Song, S.; Puzhitsky, M.; Ye, S.; Abtahi, M.; Rastogi, C. K.; Lu, E.; Hicks, G.; Manners, I.; Winnik, M. A. Crystallization-Driven Self-Assembly of Amphiphilic Triblock Terpolymers with Two Corona-Forming Blocks of Distinct Hydrophilicities. *Macromolecules* **2020**, *53* (15), 6576-6588.

(23) Yu, W.; Foster, J. C.; Dove, A. P.; O'Reilly, R. K. Length Control of Biodegradable Fiber-Like Micelles via Tuning Solubility: A Self-Seeding Crystallization-Driven Self-Assembly of Poly(ε-Caprolactone)-Containing Triblock Copolymers. *Macromolecules* **2020**, *53* (4), 1514-1521.

(24) Inam, M.; Cambridge, G.; Pitto-Barry, A.; Laker, Z. P. L.; Wilson, N. R.; Mathers, R. T.; Dove, A. P.; O'Reilly, R. K. 1D Vs. 2D Shape Selectivity in the Crystallization-Driven Self-Assembly of Polylactide Block Copolymers. *Chem. Sci.* **2017**, *8* (6), 4223-4230.

(25) Song, S.; Liu, X.; Nikbin, E.; Howe, J. Y.; Yu, Q.; Manners, I.; Winnik, M. A. Uniform 1D Micelles and Patchy & Block Comicelles Via Scalable, One-Step Crystallization-Driven Block Copolymer Self-Assembly. *J. Am. Chem. Soc.* **2021**, *143* (16), 6266-6280.

(26) Cai, J.; Li, C.; Kong, N.; Lu, Y.; Lin, G.; Wang, X.; Yao, Y.; Manners, I.; Qiu, H.

Tailored Multifunctional Micellar Brushes Via Crystallization-Driven Growth from a Surface. *Science* **2019**, *366* (6469), 1095-1098.

(27) He, X.; Hsiao, M.-S.; Boott, C. E.; Harniman, R. L.; Nazemi, A.; Li, X.; Winnik, M. A.; Manners, I. Two-Dimensional Assemblies from Crystallizable Homopolymers with Charged Termini. *Nat. Mater.* **2017**, *16* (4), 481-489.

(28) Gilroy, J. B.; Gädt, T.; Whittell, G. R.; Chabanne, L.; Mitchels, J. M.; Richardson, R. M.; Winnik, M. A.; Manners, I. Monodisperse Cylindrical Micelles by Crystallization-Driven Living Self-Assembly. *Nat. Chem.* **2010**, *2* (7), 566-570.

(29) Gadt, T.; Ieong, N. S.; Cambridge, G.; Winnik, M. A.; Manners, I. Complex and Hierarchical Micelle Architectures from Diblock Copolymers Using Living, Crystallization-Driven Polymerizations. *Nat. Mater.* **2009**, *8* (2), 144-150.

(30) Wang, X. S.; Guerin, G.; Wang, H.; Wang, Y. S.; Manners, I.; Winnik, M. A. Cylindrical Block Copolymer Micelles and Co-Micelles of Controlled Length and Architecture. *Science* **2007**, *317* (5838), 644-647.

(31) Hudson, Z. M.; Boott, C. E.; Robinson, M. E.; Rupar, P. A.; Winnik, M. A.; Manners, I. Tailored Hierarchical Micelle Architectures Using Living Crystallization-Driven Self-Assembly in Two Dimensions. *Nat. Chem.* **2014**, *6* (10), 893-898.

(32) Qiu, H. B.; Gao, Y.; Boott, C. E.; Gould, O. E. C.; Harniman, R. L.; Miles, M. J.; Webb, S. E. D.; Winnik, M. A.; Manners, I. Uniform Patchy and Hollow Rectangular Platelet Micelles from Crystallizable Polymer Blends. *Science* **2016**, *352* (6286), 697-701.

(33) Tong, Z.; Su, Y.; Jiang, Y.; Xie, Y.; Chen, S.; O'Reilly, R. K. Spatially Restricted Templated Growth of Poly(ε-Caprolactone) from Carbon Nanotubes by Crystallization-Driven Self-Assembly. *Macromolecules* **2021**, *54* (6), 2844-2851.

(34) Arno, M. C.; Inam, M.; Coe, Z.; Cambridge, G.; Macdougall, L. J.; Keogh, R.; Dove, A. P.; O'Reilly, R. K. Precision Epitaxy for Aqueous 1D and 2D Poly(ε-Caprolactone) Assemblies. *J. Am. Chem. Soc.* **2017**, *139* (46), 16980-16985.

(35) Li, Z.; Zhang, Y.; Wu, L.; Yu, W.; Wilks, T. R.; Dove, A. P.; Ding, H.-m.; O'Reilly, R. K.; Chen, G.; Jiang, M. Glyco-Platelets with Controlled Morphologies via Crystallization-Driven Self-Assembly and Their Shape-Dependent Interplay with Macrophages. *ACS Macro Lett.* **2019**, *8* (5), 596-602.

(36) He, X.; He, Y.; Hsiao, M.-S.; Harniman, R. L.; Pearce, S.; Winnik, M. A.; Manners, I. Complex and Hierarchical 2D Assemblies via Crystallization-Driven Self-Assembly of Poly(*L*-Lactide) Homopolymers with Charged Termini. *J. Am. Chem. Soc.* **2017**, *139* (27), 9221-9228.

(37) He, Y.; Eloi, J.-C.; Harniman, R. L.; Richardson, R. M.; Whittell, G. R.; Mathers, R. T.; Dove, A. P.; O'Reilly, R. K.; Manners, I. Uniform Biodegradable Fiber-Like Micelles and Block Comicelles via "Living" Crystallization-Driven Self-Assembly of Poly(*L*-Lactide) Block Copolymers: The Importance of Reducing Unimer Self-Nucleation Via Hydrogen Bond Disruption. *J. Am. Chem. Soc.* **2019**, *141* (48), 19088-19098.

(38) Finnegan, J. R.; He, X.; Street, S. T. G.; Garcia-Hernandez, J. D.; Hayward, D. W.; Harniman, R. L.; Richardson, R. M.; Whittell, G. R.; Manners, I. Extending the

Scope of "Living" Crystallization-Driven Self-Assembly: Well-Defined 1D Micelles and Block Comicelles from Crystallizable Polycarbonate Block Copolymers. *J. Am. Chem. Soc.* **2018**, *140* (49), 17127-17140.

(39) He, X.; Finnegan, J. R.; Hayward, D. W.; MacFarlane, L. R.; Harniman, R. L.; Manners, I. Living Crystallization-Driven Self-Assembly of Polymeric Amphiphiles: Low-Dispersity Fiber-Like Micelles from Crystallizable Phosphonium-Capped Polycarbonate Homopolymers. *Macromolecules* **2020**, *53* (23), 10591-10600.

(40) Hils, C.; Schmelz, J.; Drechsler, M.; Schmalz, H. Janus Micelles by Crystallization-Driven Self-Assembly of an Amphiphilic, Double-Crystalline Triblock Terpolymer. *J. Am. Chem. Soc.* **2021**, *143* (38), 15582-15586.

(41) Schmelz, J.; Schedl, A. E.; Steinlein, C.; Manners, I.; Schmalz, H. Length Control and Block-Type Architectures in Worm-Like Micelles with Polyethylene Cores. *J. Am. Chem. Soc.* **2012**, *134* (34), 14217-14225.

(42) Schmelz, J.; Karg, M.; Hellweg, T.; Schmalz, H. General Pathway toward Crystalline-Core Micelles with Tunable Morphology and Corona Segregation. *ACS Nano* **2011**, *5* (12), 9523-9534.

(43) Shaikh, H.; Jin, X.-H.; Harniman, R. L.; Richardson, R. M.; Whittell, G. R.; Manners, I. Solid-State Donor-Acceptor Coaxial Heterojunction Nanowires Via Living Crystallization-Driven Self-Assembly. *J. Am. Chem. Soc.* **2020**, *142* (31), 13469-13480.

(44) Fukui, T.; Garcia-Hernandez, J. D.; MacFarlane, L. R.; Lei, S.; Whittell, G. R.;

Manners, I. Seeded Self-Assembly of Charge-Terminated Poly(3-Hexylthiophene) Amphiphiles Based on the Energy Landscape. *J. Am. Chem. Soc.* **2020**, *142* (35), 15038-15048.

(45) Nie, J.; Wang, Z.; Huang, X.; Lu, G.; Feng, C. Uniform Continuous and Segmented Nanofibers Containing a π-Conjugated Oligo(*p*-Phenylene Ethynylene) Core via "Living" Crystallization-Driven Self-Assembly: Importance of Oligo(*p*-Phenylene Ethynylene) Chain Length. *Macromolecules* **2020**, *53* (15), 6299-6313.

(46) Ma, C.; Wang, Z.; Huang, X.; Lu, G.; Manners, I.; Winnik, M. A.; Feng, C. Water-Dispersible, Colloidally Stable, Surface-Functionalizable Uniform Fiberlike Micelles Containing a π-Conjugated Oligo(*p*-Phenylenevinylene) Core of Controlled Length. *Macromolecules* **2020**, *53* (18), 8009-8019.

(47) Ma, C.; Tao, D.; Cui, Y.; Huang, X.; Lu, G.; Feng, C. Fragmentation of Fiber-Like Micelles with a π-Conjugated Crystalline Oligo(*p*-Phenylenevinylene) Core and a Photocleavable Corona in Water: A Matter of Density of Corona-Forming Chains. *Macromolecules* **2020**, *53* (19), 8631-8641.

(48) Yang, S.; Kang, S.-Y.; Choi, T.-L. Semi-Conducting 2D Rectangles with Tunable Length Via Uniaxial Living Crystallization-Driven Self-Assembly of Homopolymer. *Nat. Commun.* **2021**, *12* (1), 2602.

(49) Ganda, S.; Wong, C. K.; Stenzel, M. H. Corona-Loading Strategies for Crystalline Particles Made by Living Crystallization-Driven Self-Assembly. *Macromolecules* **2021**, *54* (14), 6662-6669.

(50) Wang, Z.; Ma, C.; Huang, X.; Lu, G.; Winnik, M. A.; Feng, C. Self-Seeding of

Oligo(*p*-Phenylenevinylene)-*b*-Poly(2-Vinylpyridine) Micelles: Effect of Metal Ions. *Macromolecules* **2021**, *54* (14), 6705-6717.

(51) Nabiyan, A.; Biehl, P.; Schacher, F. H. Crystallization Vs Metal Chelation: Solution Self-Assembly of Dual Responsive Block Copolymers. *Macromolecules* **2020**, *53* (13), 5056-5067.

(52) Jarrett-Wilkins, C. N.; Pearce, S.; MacFarlane, L. R.; Davis, S. A.; Faul, C. F. J.; Manners, I. Surface Patterning of Uniform 2D Platelet Block Comicelles Via Coronal Chain Collapse. *ACS Macro Lett.* **2020**, *9* (11), 1514-1520.

(53) Robin, M. P.; O'Reilly, R. K. Fluorescent and Chemico-Fluorescent Responsive Polymers from Dithiomaleimide and Dibromomaleimide Functional Monomers. *Chem. Sci.* **2014**, *5* (7), 2717-2723.

(54) Xie, Y.; Arno, M. C.; Husband, J. T.; Torrent-Sucarrat, M.; O'Reilly, R. K. Manipulating the Fluorescence Lifetime at the Sub-Cellular Scale Via Photo-Switchable Barcoding. *Nat. Commun.* **2020**, *11* (1), 2460.

(55) Yu, W.; Inam, M.; Jones, J. R.; Dove, A. P.; O'Reilly, R. K. Understanding the CDSA of Poly(*L*-Lactide) Containing Triblock Copolymers. *Polym. Chem.* **2017**, *8* (36), 5504-5512.